Advancements in Electrical and Electronics Technology
Received: Feb 06, 2016, Accepted: Mar 09, 2016, Published: Mar 11, 2016
Adv Electr Electron Technol, Volume 2, Issue 1
http://crescopublications.org/aeet/AEET-2-008.pdf
Article Number: AEET-2-008

Research Article **Open Access**

Medium Voltage High-Power Converter Topology for 10MW Wind Generation with the Large Permanent Magnet Wind Generator Systems by using FUZZY Controller

A Mahaboob Basha[1*], Dawood Shaik[2] and Dr. Abdul Ahad[3]

[1]M.Tech (P.S) PG Scholar, Department of EEE, Nimra Institute of Science & Technology, Vijayawada, Andhra Pradesh, India

[2] Assistant Professor, Department of EEE, Nimra Institute of Science & Technology, Vijayawada, Andhra Pradesh, India

[3]Professor, Department of EEE, Nimra Institute of Science & Technology, Vijayawada, Andhra Pradesh, India

***Corresponding Author:** A Mahaboob Basha, M.Tech (P.S) PG Scholar, Department of EEE, Nimra Institute of Science & Technology, Vijayawada, Andhra Pradesh, India.

Citation: A Mahaboob Basha, Dawood Shaik and Dr. Abdul Ahad (2016) Medium Voltage High-Power Converter Topology for 10MW Wind Generation with the Large Permanent Magnet Wind Generator Systems by using FUZZY Controller. AdvElectr Electron Technol 2: 008.

Abstract

This paper proposes a modular, medium voltage, high- power converter topology for the large permanent magnet wind generator system, eliminating the grid-side step-up transformer, which is desirable for both onshore and offshore wind turbines. The power conversion systems for large wind turbines are facing a great challenge as today's wind turbine power outputs approach5 MW and above. The conventional low voltage power conversion system will suffer from a high transmission current, which significantly increases losses and cost of the cables as well as voltage drop. The converter modules are cascaded to achieve medium voltage output. Each converter module is fed by a pair of generator coils with 90 phase shift to get the stable dc-link power. At the grid-side, H-bridge inverters are connected in series to generate multilevel medium voltage output and the voltage- oriented vector control scheme is adopted to regulate the converter active and reactive power transferred to the grid. The power factor correction (PFC) circuit enables the generator to achieve unity power factor operation and the generator armature inductance is used as ac-side PFC boost inductance. Simulation results with a 2-MW wind turbine system and experimental results with a down-scaled 3-kW system validate the proposed topology and control methods. The proposed system can successfully deliver power from the wind generator to the grid.

I. Introduction

Today, the most popular large variable-speed wind turbinesare rated around 1.5–3 MW. Nevertheless, 7-MWwind turbines have recently appeared and even larger windturbines, e.g., 10MW, are under development in order to reducethe unit cost of wind power generation [1, 2]. Wind turbinesequipped with direct-drive permanent magnet generators(PMGs) and full power converters are generally favored due tosimplified drive train structure and thus higher reliability, especiallyfor offshore applications, compared with the doubly fedinduction generator-based system. Most of the present windgenerator and power converter systems are based on the690Vand two-level voltage–source or current–source convertersare normally used [3, 4]. The continuous increase in windturbine power ratings will generate larger current, e.g., from1673 A for 2-MW system to 8810 A for 10-MW system. Powerconverters are therefore connected in parallel to handle theincreasing current [5, 6]. Meanwhile, large current transferresults in a parallel connection of multiple power cables goingdown through the tower and causes substantial losses,voltage drop, as well as high cost of cables, switchgears, andterminal connections [7]. These disadvantages can be offset byplacing the step-up transformer (e.g., 690 V/33 kV) into thenacelle. However, the bulky and heavy transformer occupies thelimited space of the nacelle and increases the mechanical stress ofthe tower. Therefore, a medium-voltage power conversion system(e.g., 10 kV) would be more desirable for large wind powerconversion by reducing the current level and associated cablecost and losses, as well as improving the system power density.The benefits of adopting medium-voltage power conversiontechnology have been proved in motor drive applications, wheremedium-voltage (3–33 kV) configuration is generally used whenthe system power rating is higher than 1 MW [8]. Table I showsthe current rating of an exemplar 5- and 10-MW systems with690-V and 10-kV voltage level for comparison. As seen, transferringfrom low voltage (690 V) to medium voltage (10 kV) cansignificantly reduce the current level. Further, considering thehigh maintenance cost and fault-tolerant requirement especially for offshore wind applications, a modular converter and generatorstructure is even preferable.

Regarding medium-voltage multilevel converter topologiesfor wind power applications, papers [9-12] investigate the suitability of three-level neutral-point-clamped converters. Although a higher voltage rating and reduced output harmonicsare achieved, the ac-side voltage is limited to 4.0 kV if using4.5-kV integrated gate-commutated thyristors (IGCTs) [11]. The voltage rating may be further increased if using 6-kV IGCT; however, the cost and availability becomes a major concern. Afive-level hybrid converter topology with increasing number of devices is presented into further increase the converter voltage and power capability [13]. However, the reliability restricts itsapplication. If one device fails, the whole converter systemoperation may be interrupted. A more applicable way to achieve6- or 10-kV medium-voltage power conversion is through thecascaded modular converter structure [2, 8]. The voltage levelcan be easily scaled up by cascading more converter cells. Papers[14 - 18] have proposed various converter topologies based onthis concept. However, the fundamental connections betweenthese topologies are not analyzed. The cascaded convertertopology has intrinsic fault-tolerant operation capability. If onecell fails, it can be bypassed and the rest healthy cells can keepoperation [17]. One of the main disadvantages of the cascadedConverter topology is the large dc-link capacitor required to filterthe dc-link voltage ripple from the H-bridge side in each cell [14-19]. The dc-link capacitor is unreliable and is not favored inwind power applications where maintenance cost is very high.There are no effective solutions to significantly reduce the dc-linkcapacitor. In motor drive applications, diode rectifiers arenormally used, which cannot be actively controlled to compensatethe ripple power thus reducing the dc-link capacitor.

Table I: Wind turbine current rating for different voltage levels

Wind turbine power (MW)	Voltage (kV)	Current (A)
5.0	0.69	4400
	10	303
10	0.69	8810
	10	607

In this paper, a fundamental rule to construct multi-levelmodular high power converters for large wind turbine powerconversion is proposed. Based on this, three potential multi-levelmodular wind power converter topologies have been derivedusing a generalized approach for an exemplar 10-kV, 10-MWwind turbine. A special focus has been given to the topologycomprising a 10-kV generator, a multilevel modular converter,and a multi-winding grid-side transformer. A solution to reducethe dc-link capacitor is proposed by compensating the ripplepower from the three-phase grid-side inverter. A resonant controlleris presented to achieve this purpose. The current harmonicsinduced in the inverter and transformer secondary windingsby the proposed control scheme and their impact are alsoinvestigated analytically. The converter topology and dc-linkcapacitor reduction strategy has been simulated and validatedwith a 10-kV, 10-MW wind power conversion system, where thedc-link voltage ripple is effectively attenuated without affectingthe grid power quality.

II. 10-kV, 10-MW Wind Power Modular Converter Topologies

As mentioned, one of the most applicable and economic wayto achieve a 10-kV power conversion system is through seriesconnection of modular converter cells. In particular, 3.3-Kvinsulated-gate bipolar transistor (IGBT) device is considered inthis application due to their better availability and lower cost,compared with 4.5- and 6-kV devices. Figure 1 shows a generalizedphase leg of a cascaded modular converter structure. The outputsof several converter cells (ac/dc/ac) are connected in series toachieve high-voltage output. With 3.3-kV IGBTs, 10-kV linevoltageoutput can be achieved with five stages, where eachmodule dc-link voltage is regulated at around 1800 V, thus3.3-kV devices can be used. It should be noted that the convertermodules in Figure 1 cannot be directly connected in series at bothends without isolation. A galvanic isolation is needed in eachconverter module in order to cascade the outputs at either end.There are three possible locations to place the isolation, viz., atthe generator side (I), in the dc link (II), or at the grid side (III), asshown in Figure 1. The isolation can be achieved through eithergenerator isolated windings, high-frequency transformer in thedc-link or multi-winding grid-side transformer. Based on this,three potential high-power, medium-voltage modular wind convertertopologies are given in Figures 2–4, respectively.

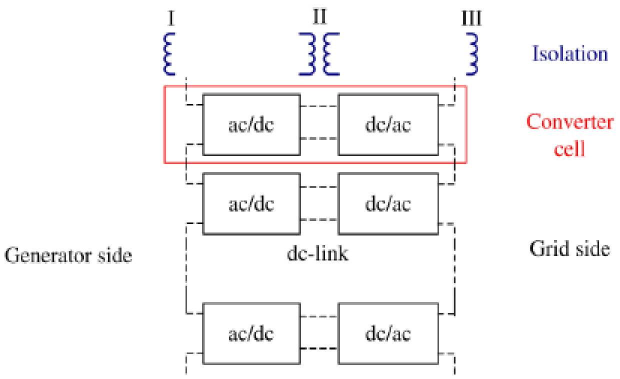

Figure 1: Generalized cascaded multilevel converter topology (one phase leg).

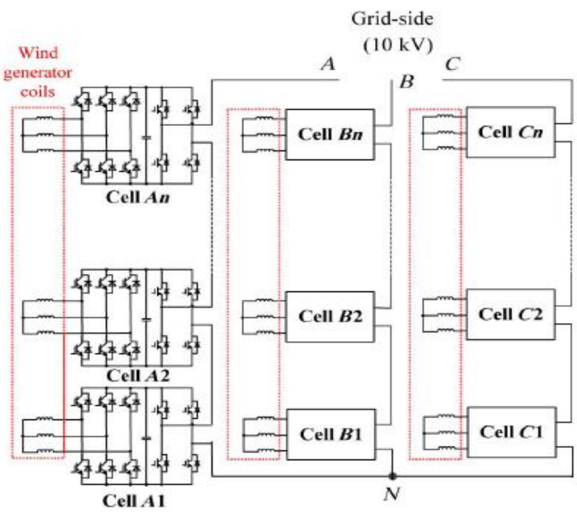

Figure 2: High-power, medium-voltage (10 kV) modular wind converter withgenerator-side isolation (converter type I).

Figure 2 shows a high-power, medium-voltage (10 kV) windconverter topology (type I) by using the generator-side isolation.The isolated coils in the generator stator windings are connectedout separately to provide independent power sources for eachconverter cell. The input power stage of each cell is a three-phaseactive rectifier and the output stage is an H-bridge inverter. Theoutputs of each H-bridge are connected in series to achieve highvoltage (e.g., 10 kV) at the grid side. This topology requires thegenerator to provide multiple three-phase coils. The direct-drivePMGs generally have many pole pairs, where the correspondingthree-phase coils of each pole pair (or several pole pairs connectedin series or in parallel, depending on the required voltagerating) can be connected out separately to meet this requirement.Regarding the control, the input three-phase rectifier is responsiblefor regulating the dc-link voltage of each converter cell andthe grid-side cascaded H-bridge converter regulates the activepower [e.g., for maximum power point tracking (MPPT)] andreactive power fed into the grid [14-16]. With this topology, thegenerator and converter are suggested to put on top of the windtower.

A step-up transformer from 10 kV to the voltage level(e.g., 33 kV) of the collection point of the wind farm may berequired and can be placed at the bottom of the tower. Alternatively,a transformer-less structure may be enabled if the numberof cascaded stages can be increased to directly meet the collectionpoint voltage. It should be noted that the increased number ofgenerator terminal connections may add extra labor and maintenancecost. A dedicated generator design and wire connectionarrangement may be required.

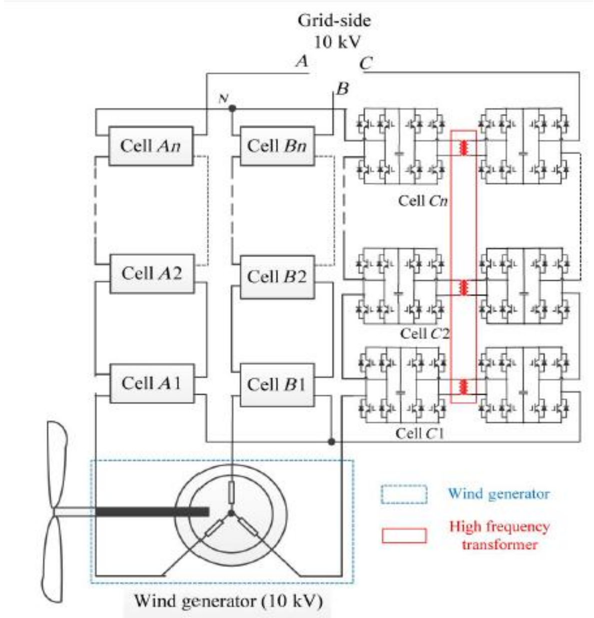

Figure 3: High-power, medium-voltage (10 kV) modular wind converter with highfrequencytransformer isolation (converter type II).

Figure 3 shows a second wind converter topology (type II) with ahigh-frequency transformer as the isolation, which is insertedinto the dc link together with a back-to-back H-bridge converter.This high-frequency isolation unit is also called dual activebridge (DAB) converter, where the two H-bridge converters atboth sides of the high-frequency transformer operate at a higherfrequency (e.g., several kHz), thus the size and weight of thetransformer can be significantly reduced compared with the linefrequency(50 or 60 Hz) transformer [20, 21]. The input andoutput stages of each converter cell are H-bridge converters (withthe DAB converter in between). A standard three-phase 10-kVgenerator is used and the H-bridge converters are cascaded atboth the generator side and grid side to achieve 10-kV voltagecapability thus regulating the generator and grid power. The turnsratio of the high-frequency isolation transformer can be adjusted(1:1 or 1: *n*) to achieve the desired voltage level. The powerconverter can be put flexibly either on top of the tower or at thebottom since 10-kV voltage is achieved at both ends of theconverter. The main concern with this topology is the extra lossescaused by the inserted DAB converter and high-frequencytransformer, which may be mitigated by using advanced magneticsmaterial, soft-switching topologies and new wide-bandgappower devices, e.g., silicon-carbide (Sic) based device.

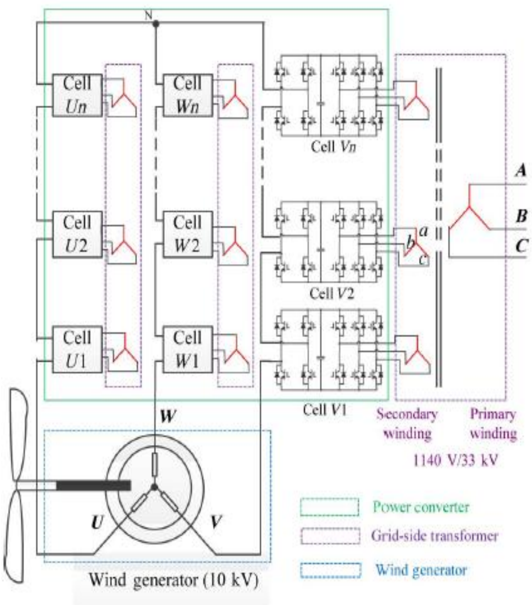

(a)

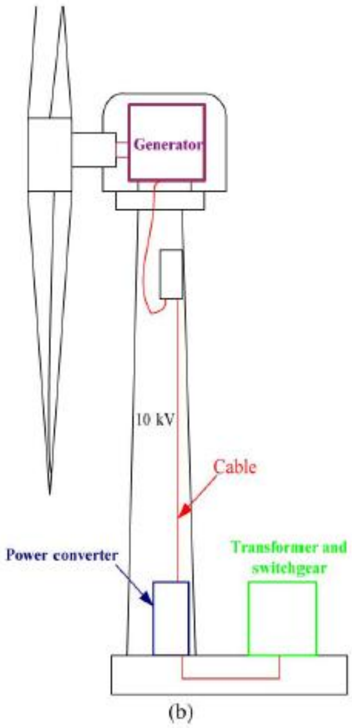

Figure 4: High-power, medium-voltage (10 kV) modular wind converter with gridsidetransformer isolation (converter type III): (a) generator and converterstructure and (b) wind turbine electrical configuration.

Figure 4(a) shows another high-power, medium-voltage windconverter topology (type III) with a grid-side isolation transformer,which will be further investigated in this paper. As can beseen, this topology adopts a standard 10-kV wind generator and agrid-side step-up transformer with multiple secondary windings(1140 V/33 kV), which provides isolation of each converter celland also boosts the converter voltage to the grid voltage of 33 kV.The power converter and the transformer can be put at the bottomof the tower as shown in Figure 4(b), which reduces the mechanicalstress of the tower and saves the space in the nacelle. The inputstage of each converter cell is an H-bridge rectifier which is thenconnected in series to achieve 10-kV voltage capability to controlthe generator. The output stage of each converter cell is a threephaseinverter and is connected to the transformer secondarywindings, responsible for regulating the dc-link voltage. Similarto the previous two topologies, this modular structure benefitsfrom fault-tolerant capability, when one cell fails, it can bebypassed by a switch connected in parallel to the H-bridgeconverter output and the remaining health cells can still maintainoperation subject to the reduce of power output. In view ofthe successful applications of the cascaded H-bridge converterin high power motor drive area, this topology may become astrong candidate for future large wind turbine power conversionsystems [22].

It should be noted that the low-frequency single-phase fluctuatingpower at the input stage of each cell (H-bridge) in Figure 4(a)will cause dc-link voltage ripple, which gets larger with lowergenerator stator frequency and higher power level. For variablespeed,direct-drive PMGs, the stator frequency is generally low(e.g., below 15 Hz). Therefore, large dc-link capacitance isrequired to smooth out the voltage ripple appeared on the dclink, which are bulky and significantly increase the system cost aswell as cause reliability issues due to the lifetime of electrolyticcapacitors. This issue also happens to the other two topologies inFigures 2 and 3. In Section IV, a solution to reduce the dc-linkcapacitance will be introduced in a later session.

III. 10-MW Wind Turbine Specifications and Converter Control Strategy

III-PI Controller

Proportional – Integral-Derivative controller (PIDcontroller) is a control loop feedback mechanism(controller) widely used in industrial control systems and its block diagram is shown in Figure 6. A PID controllercalculates an error value as the difference between ameasured process variable and a desired setpoint. Thecontroller attempts to minimize the error by adjusting theprocess through use of a manipulated variable.

The PID controller algorithm involves threeseparate constant parameters, and is accordingly sometimescalled three-term control: the proportional, the integral andderivative values, denoted P, I, and D.

Some applications may require using only one or twoactions to provide the appropriate system control. This isachieved by setting the other parameters to zero. A PIDcontroller will be called a PI, PD, P or I controller in theabsence of the respective control actions. PI controllers arefairly common, since derivative action is sensitive tomeasurement noise, whereas the absence of an integral termmay prevent the system from reaching its target value due tothe control action.

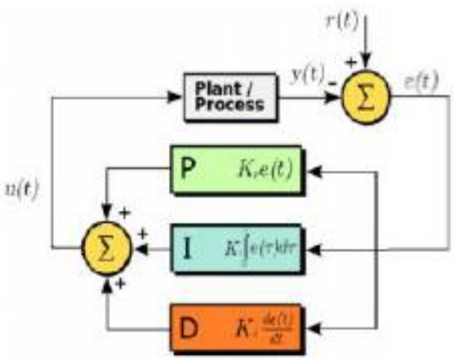

Figure 6: A block diagram of a PID controller in a feedbackloop

Most modern PID controllers in industry areimplemented in programmable logic controllers (PLCs) oras a panel-mounted digital controller. Softwareimplementations have the advantages that they are relativelycheap and are flexible with respect to the implementation ofthe PID algorithm. PID temperature controllers are appliedin industrial ovens, plastics injection machinery, hotstamping machines and packing industry.

The PID control scheme is named after its threecorrecting terms, whose sum constitutes the manipulatedvariable (MV). The proportional, integral, and derivativeterms are summed to calculate the output of the PIDcontroller. Defining $u(t)$ as the controller output, the finalform of the PID algorithm is:

$$u(t) = MV(t) = K_p e(t) - K_i \int_0^t e(\tau)\, d\tau + K_d \frac{d}{dt} e(t)$$

Where Kp: Proportional gain, a tuning parameter
Ki: Integral gain, a tuning parameter
Kd: Derivative gain, a tuning parameter
: Error =SP-PV
t: Time or instantaneous time (the present)
τ : Variable of integration; takes on values from time 0 tothe present t.

There are so many methods to calculate the values of Proportional gain (Kp),Integral gain(Ki),Derivative gain(Kd).One among them is described as follows:

Ziegler–Nichols method

Another heuristic tuning method is formally known as theZiegler–Nichols method, introduced by John G. Ziegler andNathaniel B. Nichols in the 1940s. As in the method above,the K_i and K_d gains are first set to zero. Theproportional gain is increased until it reaches the ultimategain, K_u, at which the output of the loop starts to oscillate. K_u and the oscillation period P_u are used to set the gainsas shown:

Ziegler–Nichols method

Control Type	K_p	K_i	K_d
P	$0.50K_u$	-	-
PI	$0.45K_u$	$1.2K_p/P_u$	-
PID	$0.60K_u$	$2K_p/P_u$	$K_pP_u/8$

These gains apply to the ideal, parallel form of the PIDcontroller. When applied to the standard PID form, theintegral and derivative time parameters T_i and T_d are onlydependent on the oscillation period P_u.

A PI Controller (proportional-integral controller) is aspecial case of the PID controller in which the derivative(D) of the error is not used as shown in Figure 7.

The controller output is given by

$$K_P\Delta + K_I \int \Delta\, dt$$

WhereΔ is the error or deviation of actual measured value(PV) from the setpoint (SP).

$$\Delta = SP - PV.$$

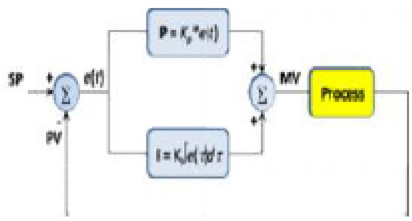

Figure 7: Basic block of a PI controller

A PI controller can be modeled easily in softwaresuch as Simulink or Xcos using a "flow chart" box involvingLaplace operators:

$$C = \frac{G(1 + \tau s)}{\tau s}$$

Where

$G = K_{P=}$ Proportional gain

$G/\tau = K_{I=}$ Integral gain

Setting a value for*G* is often a tradeoff betweendecreasing overshoot and increasing settling time.

The lack of derivative action may make the systemmore steady in the steady state in the case of noisy data.This is because derivative action is more sensitive to higherfrequencyterms in the inputs. Hence the PI controllercontrols the voltage error between the reference voltage andmean voltage of system by controlling the duty cycles ofsemiconductor devise.

IV Fuzzy Logic Controller

The basic concept in FL, which plays a central role in most of its applications, is that of a fuzzy if-then rule or,simply, fuzzy rule. Although rule-based systems have a longhistory of use in Artificial Intelligence (AI), what is missingin such systems is a mechanism for dealing with fuzzyconsequents and fuzzy antecedents. In fuzzy logic, thismechanism is provided by the calculus of fuzzy rules. Thecalculus of fuzzy rules serves as a basis for what might becalled the Fuzzy Dependency and Command Language (FDCL). In most of the applications of fuzzy logic, a fuzzylogic solution is, in reality, a translation of a human solutioninto FDCL.First-generation simple fuzzy logic controllerscan generally be depicted by a block diagram in Figure 8.

The knowledge-based module contains knowledgeabout all the input and output fuzzy partitions. It will

Include the term set and the corresponding membershipfunctions defining the input variables to the fuzzy rule-basesystem and the output variables, or control actions, to theplant under control.

Type of membership function. In this paper the suggestedmembership function is triangular and the rules are made.The definition of a membership function: A graph thatdefines how each point in the input space is mapped tomembership value between 0 and 1. Input space is oftenreferred as the universe of discourse or universal set (u),which contain all the possible elements of concern in eachparticular application.

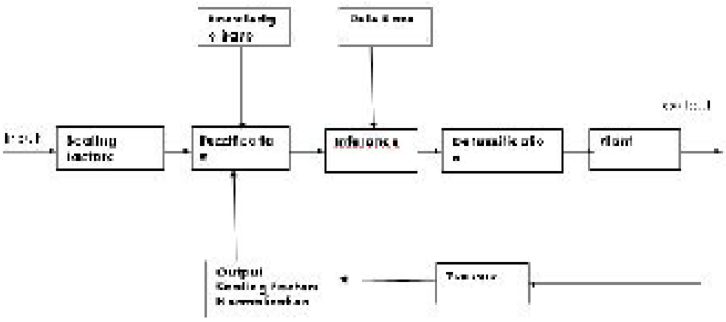

Figure 8: A Simple Fuzzy Logic Control System

Before we start defining different types ofmembership functions, let us consider a Fuzzy IF-THENrule for a car:

IF the speed of a car is high, THEN apply less force to theaccelerator

IF the speed is low, THEN apply more force to theAccelerator

Triangular: This is formed by the combination of straightlines. The function is name as “trimf”.We consider theabove case i.e. fuzzy set Z to represent the “number close tozero”. So mathematically we can also represent it as

0 if x<-1

μz(x) = x + 1 if -1 ≤ x <0 (1.4)

1 –x if 0 ≤ x <1

0 if 1≤ x

Figure (9) called “triangular membership function”

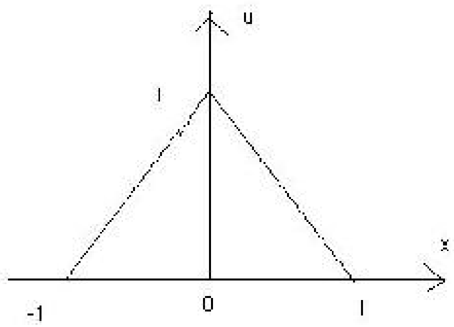

Figure 9: Triangular Membership Function

By using this membership function, a group ofrules are obtained according to the inputs. These rules areprogrammed and stored as a .fis file, which imported to theworkplace to run.

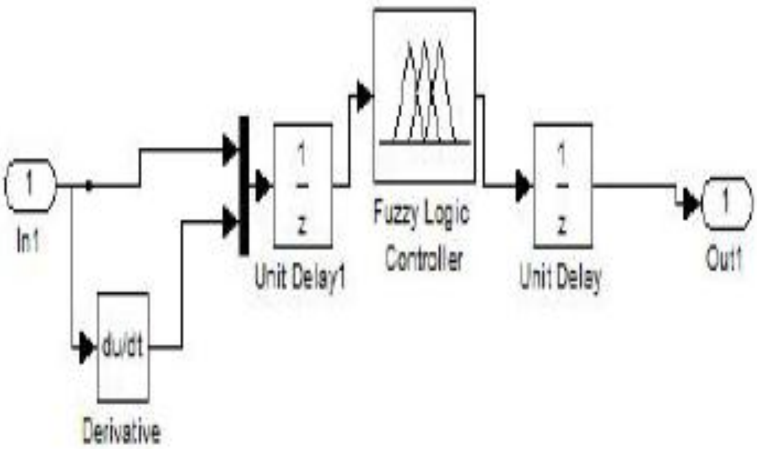

A. FUZZY Controller

A 10-kV, 10-MW wind turbine and its PMG parameters aredesigned. The rated speed of the wind turbine is 10 rpm at windspeed of 12 m/s [23]. The PMG has 90 pole pairs, correspondingto 15-Hz stator frequency at rated speed. Figure 5 shows thecaptured wind power variation with the generator speed. Thewind turbine control should aim to capture maximum windpower by regulating the generator speed/power following MPPTunder normal conditions.

B. Generator and Cascaded H-Bridge Converter Control Strategy

The wind generator (PMG) shown in Figure 4(a) can be modeledin a synchronous rotating (,) frame [3], [24]. With rotor fluxorientedcontrol, the PMG torque can be controlled by the –axiscurrent, while the -axis current is controlled to maximize thegenerator efficiency. In order to achieve MPPT, the generatortorque reference is set as the product of the optimal coefficientand the square of generator speed [25]. The standard phaseshiftedpulse width modulation (PWM) is adopted to modulatethe cascaded H-bridge converters, thus generating the requiredvoltage according to the voltage reference.

C. Grid-Side Inverter Model and Control Strategy

At the grid side, the three-phase inverter in each converter cellas shown in Figure 4(a) is responsible for regulating the convertercell dc-link voltage, transferring the active power generated fromwind generator to the grid. Since the inverter current is activelycontrolled to be sinusoidal, the topology in Figure 4(a) does not need multiple phase-shifted transformer secondary windings(Zigzag winding) for harmonics reduction as the case in motordrive applications with diode rectifier, leading to a simplifiedtransformer design. The transformer leakage inductance can befurther used as the filter inductance. The model of the grid-sidethree-phase inverter in each cell on frame is given asfollows [3, 14]:

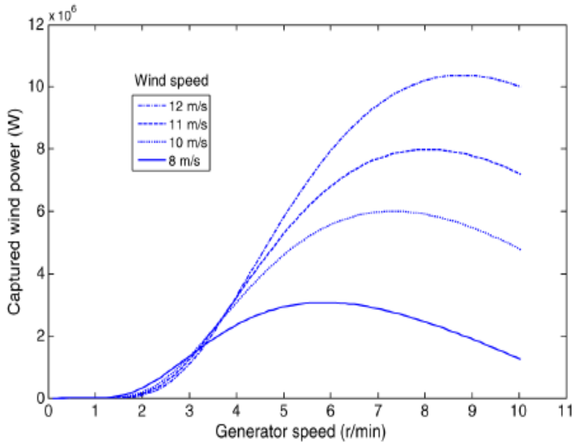

Figure 5: Variation of captured wind power with generator speed under differentwind speeds.

$$\begin{cases} L_e \frac{di_d}{dt} = -R_e i_d + \omega_e L_e i_q - S_d + u_d \\ L_e \frac{di_q}{dt} = -R_e i_q - \omega_e L_e i_d - S_q + u_q \end{cases} \quad (1)$$

Where*Le* and*Re* are the transformer leakage inductance andresistance;*u*d,*uq*,*id*,*iq* are the voltages and currents on thetransformer secondary side in the*d*,*q* frame, respectively; are the output voltages of the three-phase inverter in the switchingaverage model; andωe is the grid line frequency.

If the -axis of the rotating frame is aligned to the transformersecondary voltage vector, then*uq=0* and *u*d=E where E isthe amplitude of the transformer secondary voltage. The converteractive powerP and Qreactive power can be formulated by

$$\begin{cases} P = \frac{3}{2}(u_d i_d + u_q i_q) = \frac{3}{2} E i_d \\ Q = \frac{3}{2}(u_d i_q - u_q i_d) = \frac{3}{2} E i_q. \end{cases} \quad (2)$$

As seen, the active and reactive power flowing into the grid canbe controlled by -axis and -axis currents independently. Thegrid-side three-phase inverter control diagram is shown in Figure 6.The outer loop is the dc-link voltage control loop which is kept tobe 1800 V and inner loops are -axis and -axis current controlloops. The -axis current can be used to provide reactive power tothe grid when required subject to the current capability of theconverter.

IV. Converter Dc-Link Voltage Ripple Reduction

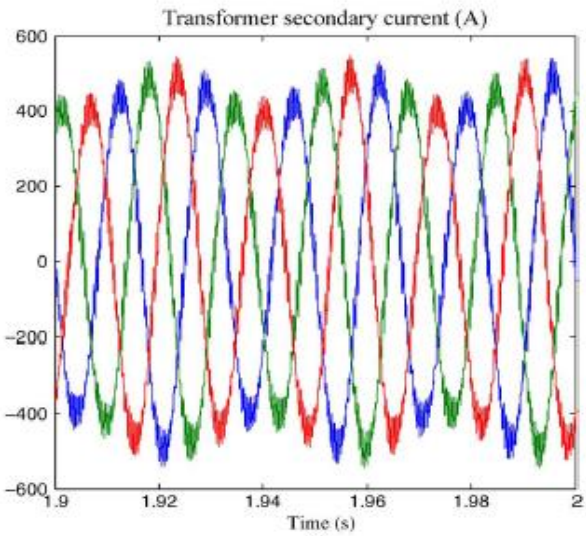

(a)

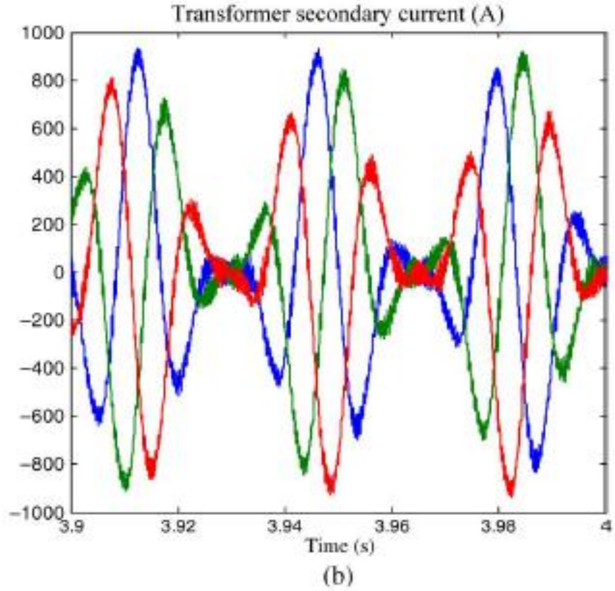

Figure 9: Inverter (transformer secondary) current with and without resonantcontroller applied: (a) without resonant controller and (b) with resonantcontroller.

C. Inverter and Transformer Power Losses Analysis

While the low-frequency power ripple from H-bridge side canbe effectively compensated from the transformer-side inverter,the harmonic current may cause extra thermal stress to theinverter power devices and the transformer secondary windings.Figure 9 shows the simulated inverter current waveform with andwithout the dc-link voltage ripple reduction method applied for a10-MW system at a rated wind speed. As seen, with the dc-linkripple reduction method applied, the peak current (due to theharmonics) of each phase may double the value of the currentwithout compensation. The exact expression of the currentwaveform is given in (13)–(15) for phase. Therefore, thepower device current rating should be chosen to meet the peakcurrent requirement.

In order to evaluate the thermal performance and the impact ofthe control algorithm on the inverter, the inverter losses anddevice junction temperature are calculated and simulated. For a10-MW, 10-kV generator, the rated root mean square (RMS)current is 577 A. With a 1140-V/33-kV grid-side transformer and15 converter cells, the transformer secondary winding RMScurrent is 337 A. Note that if the ripple power compensationscheme is activated, the peak of transformer secondary currentmay increase to 950A. With these current values, IGBT modulesfrom infineon FZ1000R33HL3 (3300 V, 1000 A) are used forboth H-bridge rectifier and the inverter to evaluate the systemthermal performance [29, 30]. The switching frequency isselected at 2 kHz.

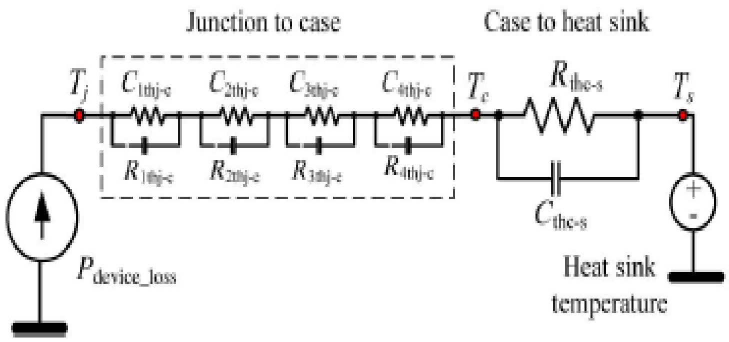

Figure10: Thermal network to evaluate the device junction temperature.

In the simulation, the heat sink temperature is assumed to befixed at 80°C due to its large thermal time constant. The thermalnetwork is shown in Figure 10. The thermal network comprises thejunction to case and case to heat sink thermal impedance.

Figure 11 shows the inverter device junction temperature variation.Without ripple power compensation, the IGBT temperaturevaries between 96 and 102°C. The diode junction temperaturevaries between 94.5 and 104°C. When the ripple power compensationscheme is applied, the inverter current becomes as inFigure 9(b) and the junction temperature variation gets larger as wellas the peak temperature, although the average temperature stayssimilar with the non-compensated case. Larger junction temperaturevariation may reduce the lifetime of the power device. Thethermal design should also make sure the peak temperaturedoes not exceed the maximum allowable junction temperature.

Another impact of the ripple power compensation scheme isthe circulating harmonic current inside the transformer secondarywindings and the corresponding extra copper losses it hasintroduced. From (13), the RMS value of the transformer secondarycurrent with harmonics can be calculated as

$$I'_{a\_\mathrm{RMS}} = \frac{V_{om} I_{om}}{3E} \cdot \sqrt{\left(\frac{1}{\sqrt{2}}\right)^2 + \left(\frac{1}{2\sqrt{2}}\right)^2 + \left(\frac{1}{2\sqrt{2}}\right)^2} = \frac{V_{om} I_{om}}{3E} \cdot \frac{\sqrt{3}}{2} \quad (17)$$

WhereI'a_RMS is the RMS value of the current including harmonics.The RMS value of the fundamental current can be calculatedas

$$I_{a\_\mathrm{RMS}} = \frac{V_{om} I_{om}}{3E} \cdot \frac{1}{\sqrt{2}}. \quad (18)$$

Therefore, the ratio of the transformer secondary copper losswith and without the ripple power compensation scheme cans becalculated as

$$\left(\frac{I'_{a\_\mathrm{RMS}}}{I_{a\_\mathrm{RMS}}}\right)^2 = \left(\frac{\sqrt{6}}{2}\right)^2 = 1.5. \quad (19)$$

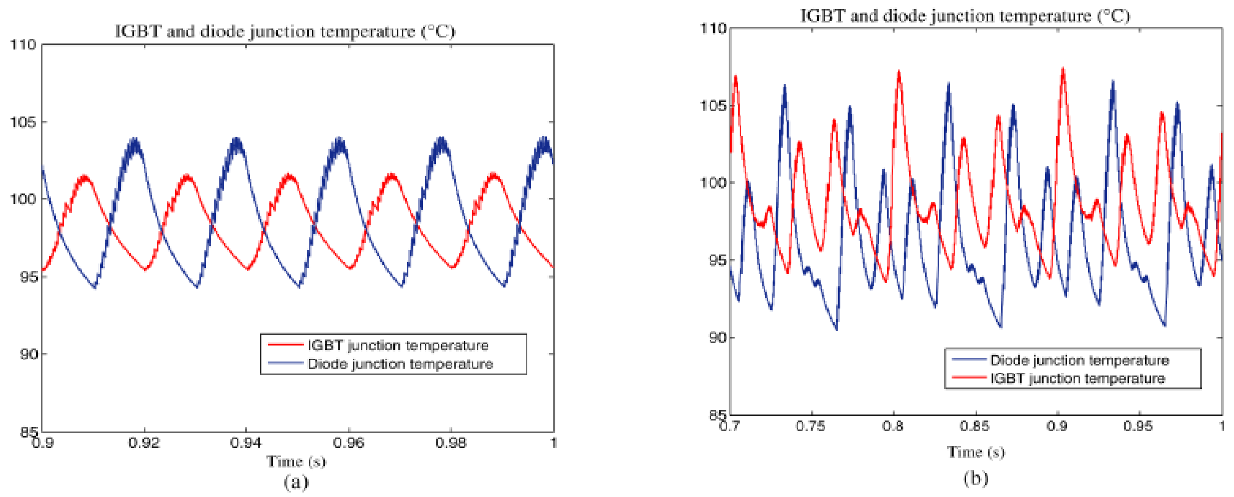

Figure 11: Inverter device (IGBT/diode) junction temperature variation: (a) withoutresonant controller and (b) with resonant controller.

As seen, the winding copper losses have increased by 50% dueto the extra harmonics, which need to be taken into considerationduring the transformer and cooling system design.

V. Simulation and Results

A simulation model has been built in MATLAB/Simulink inorder to validate the converter topology in Figure 4 and controlstrategy in Figure 6. The power converter consists of 5 stages(15 cells), with each dc-link voltage of 1800 V. The dc-linkcapacitance is 44 mF. The wind turbine characteristics are thesame as in Figure 5.

Figure 12 shows the steady-state simulation results at thewind speed of 12 m/s with 10-MW wind power generation.Figure 12(a) shows the generator-side converter output voltage,which has 11 levels and the generator current. Figure 12(b)shows the transformer secondary winding (inverter) currents(1140-V side) in one converter cell. The grid (33 kV) phaseVoltage and current are shown in Figure 12(c). As seen, the gridcurrent is kept sinusoidal and the phase relationship betweenvoltage and current indicates wind power is fed into the grid.Figure 12(d) shows the dc-link voltage regulated at 1800 V.With 44-mF dc-link capacitor, the voltage ripple is around90 V, which agrees with the calculated results by (4). A detailed waveform is shown at the bottom of this figure andthe ripple frequency is 30 Hz, which is twice of the generatorfrequency of 15 Hz.

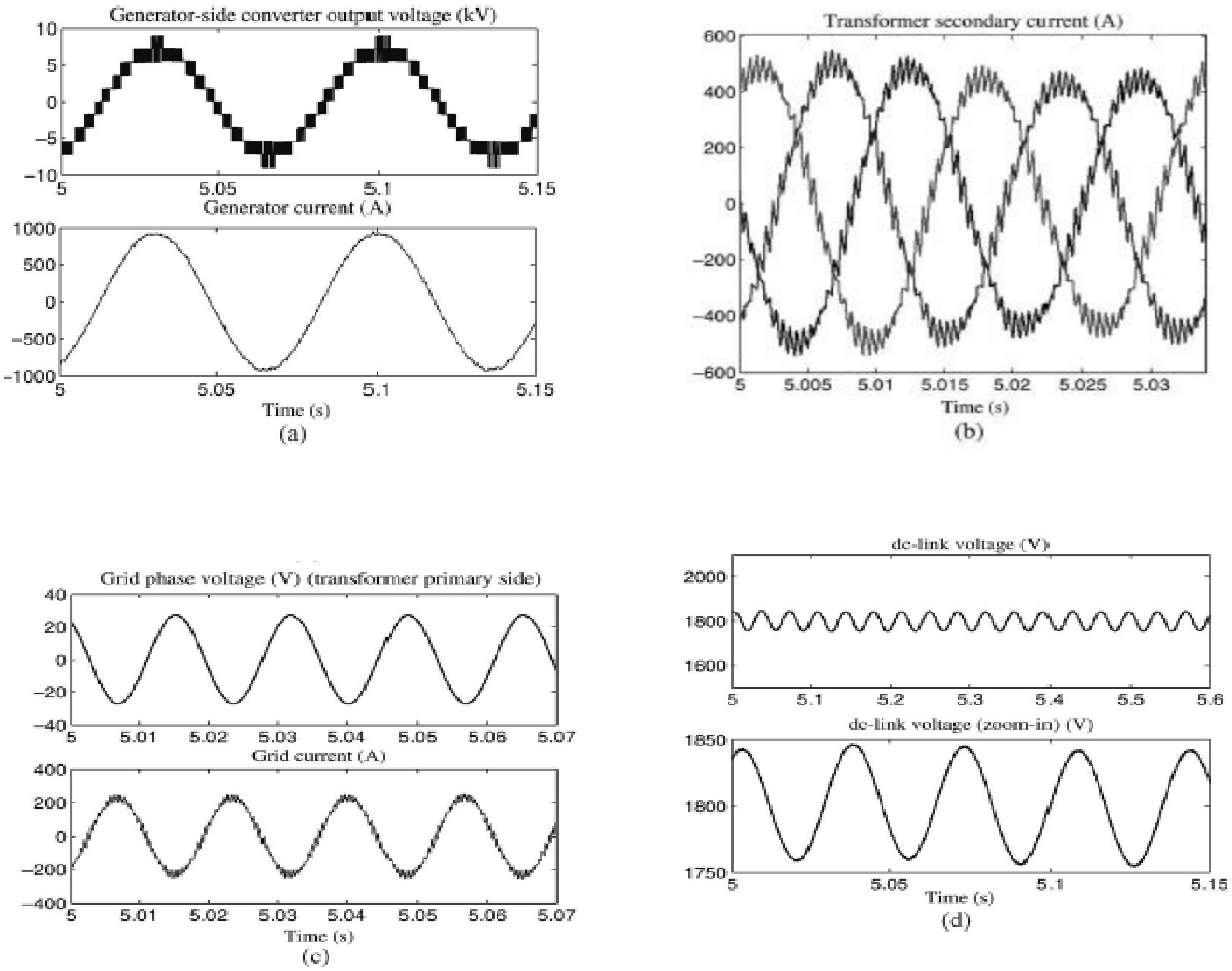

Figure 12: Steady-state simulation results at wind speed of 12 m/s: (a) generatorsideconverter output voltage and generator current, (b) transformer secondarywinding current in a converter cell, (c) grid phase voltage and current, and(d) dc-link voltage and detailed trace.

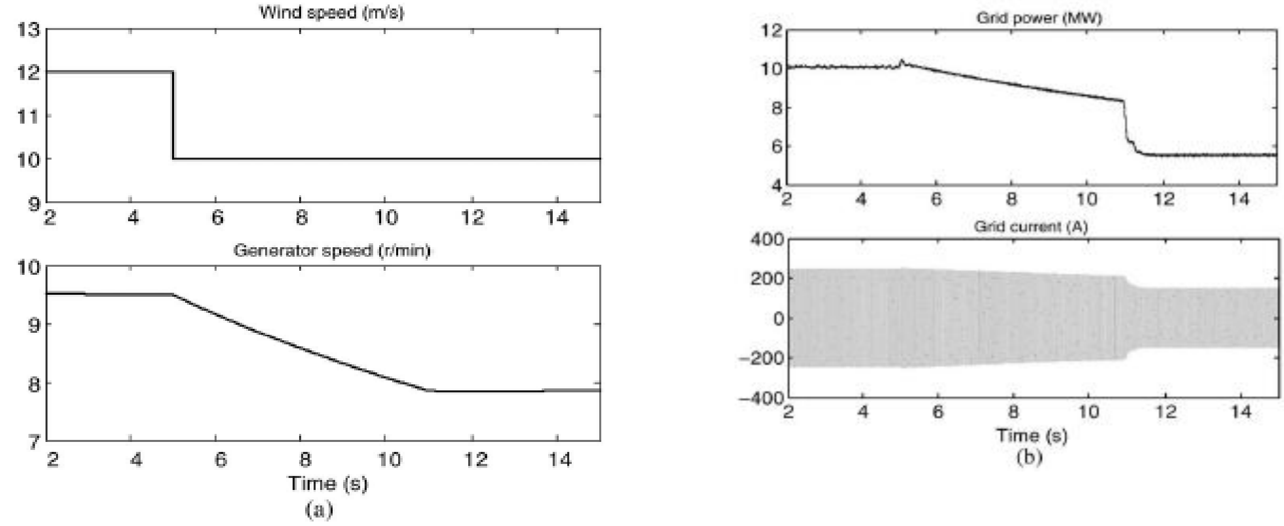

Figure 13: System response during wind speed drop from 12 to 10 m/s: (a) windspeed and generator speed and (b) power transferred to the grid and grid current.

Figure 13 shows the system response during a wind speed dropfrom 12 to 10 m/s at 5s. The converter and generator control aimsto achieve MPPT under both wind speeds. Figure 13(a) shows thewind speed profile and the corresponding generator speed. Asseen, the generator speed reduces from 9.5 (MPPT point for12 m/s) to 7.7 r/min to reach the MPPT point according to Figure 5.Figure 13(b) shows the power transferred to the grid and the gridcurrent.

Figure 14 shows the results of dc-link voltage ripple reductionby using the PIR controller in the dc-link voltage and currentcontrol loops of each converter cell, as illustrated in thediagram in Figure 6. To observe the effect more clearly, thedc-link capacitance has been reduced from 44 to 22 mF.Therefore, without using PIR controller, the dc-link voltageripple of each cell should be 180 V. Figure 14(a) shows the dc-linkvoltage, where the resonant controller is applied at 2 s.

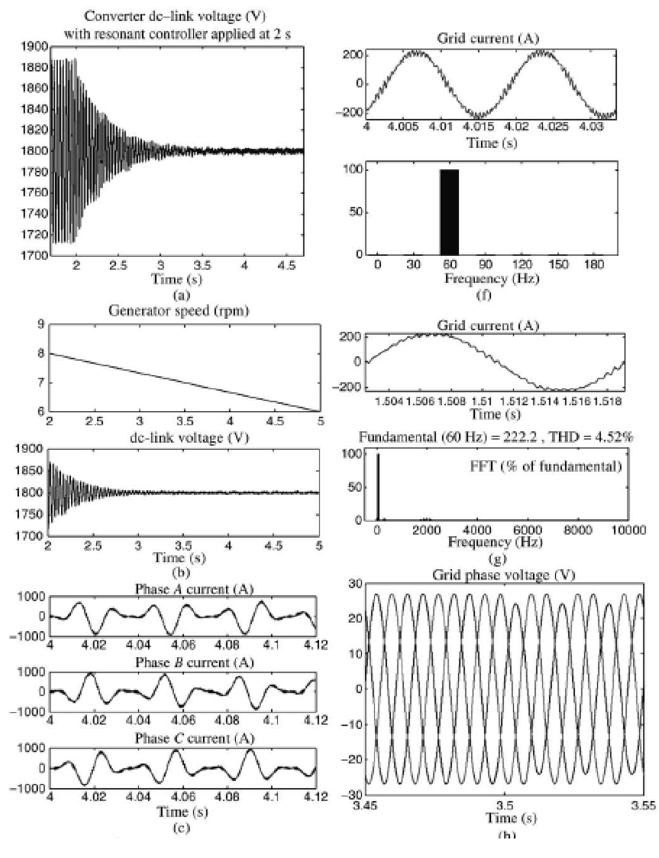

(h)

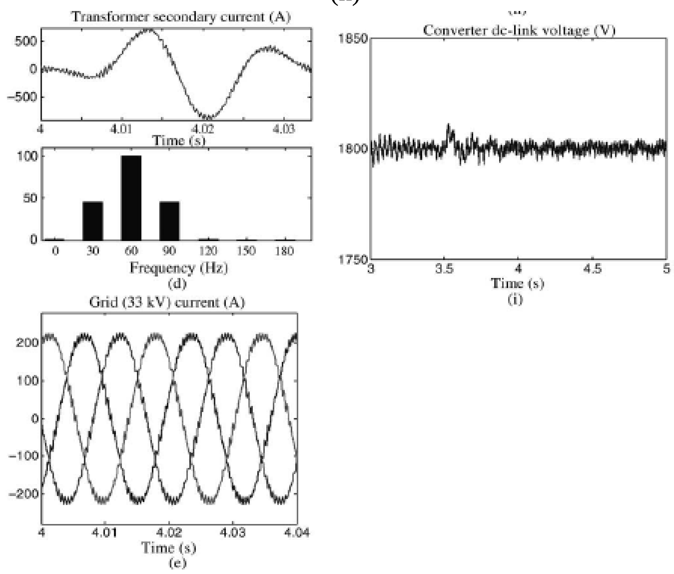

Figure 14: Simulation results with a PIR controller engaged to reduce the dc-linkvoltage ripple: (a) converter cell dc-link voltage with resonant controller appliedat 2 s, (b) dc-link voltage during generator speed variation, (c) transformersecondary winding current, (d) FFT analysis of transformer secondary windingcurrent, (e) transformer primary (grid) current, (f) FFT analysis of transformerprimary winding current, (g) THD of the grid current, (h) grid phase voltageswith phase *A*10% drop at 3.5 s, and (i) converter dc-link voltage underunbalanced grid.

AsSeen, before the resonant controller is applied, the dc-link voltage ripple is around 180 V. After the resonant controller is applied, the dc-link voltage ripple reduces dramatically to around zero, which validates the proposed dc-link voltage ripple reduction method. As a result, the required dc-linkcapacitor can be much smaller than that without a resonantcontroller, which can save the capacitor cost, size, as well asincrease the system reliability. Figure 14(b) further shows theperformance of the controller during the change of generatorspeed. The resonant controller is applied at 2s. During 2–5 sthe generator speed varies from 8 to 6 rpm and the controllereffectively adjusts the resonant frequency and attenuates thevoltage ripple regardless of the generator speed variation.Figure 14(c) shows the corresponding transformer secondarycurrent in each cell when the resonant controller is engaged.As seen, the currents are not sinusoidal due to the compensationof the pulsation power. As analyzed in (13)–(15), thecurrent contains harmonics with frequency of $\omega e + 2\omega o$ and $\omega e - 2\omega o$. The fast Fourier transform (FFT) analysis ofthe current is shown in Figure 14(d),where the current contains thegrid-frequency (ωe) component of 60 Hz as well as two otherfrequency components of 90 Hz ($\omega e + 2\omega o$) and 30 Hz( ) at the generator stator frequency ($\omega e - 2\omega o$) of 15 Hz.Figure 14(e) shows the transformer primary (grid)-side currentwaveform, which is sinusoidal and does not contain anylow-frequency harmonics as indicated by the FFT analysis inFigure 14(f) that only the 60-Hz grid-frequency componentappears. It is evident that the proposed dc-link voltage ripplereduction method does not affect the grid-side power quality.Figure 14(g) shows the total harmonic distortion (THD) of the gridcurrent, which is 4.52% in this case, where the grid-interfaceinductance is 0.5 mH and the switching frequency is 2 kHz.Figure 14(h) and (i) show the effectiveness of the dc-link voltageripple reduction scheme under an unbalanced grid condition. At3.5 s, phase*A* voltage has a 10% voltage drop. From theconverter dc-link voltage, it can be seen that the dc-link voltageripple is effectively attenuated regardless the voltage drop in phase*A*.

VI. Conclusion

In this paper, three high-power medium-voltage (10 kV)modular wind power converter topologies have been derivedbased on a generalized structure by using different formats ofisolation. A method has been proposed to attenuate the dc-linkvoltage ripple, thus reducing the capacitor requirement,by compensating the low-frequency power ripple. A PIRController-based control loop has been designed to achievethis purpose. The proposed dc-link voltage reduction schemewill introduce harmonics in the transformer secondary current;however, not degrading the grid power quality (sinusoidalcurrent). The current harmonics will increase the stress ofthe power devices and the transformer copper loss. Simulationresults with a 10-kV, 10-MW system have validated theconverter topology and control scheme. The proposed dc-linkvoltage ripple reduction method may also be used in the othertwo topologies presented in the paper.

Acknowledgment

The author would like to thank Dr. D. Grant, Visiting Fellow atthe University of Bristol, for his comments on the paper.

References

[1] M. Liserre, R. Cardenas, M. Molinas, and J. Rodriguez, "Overview of multi-MW wind turbines and wind parks," IEEE Trans. Ind. Electron., vol. 58,no. 4, pp. 1081–1095, Apr. 2011.
[2] F. Blaabjerg, M. Liserre, and K. Ma, "Power electronics converters for windturbine systems," IEEE Trans. Ind. Appl., vol. 48, no. 2, pp. 708–719,Mar. 2012.
[3] M. Chinchilla, S. Arnaltes, and J. Burgos, "Control of permanent-magnetgenerators applied to variable-speed wind-energy systems connected to thegrid," IEEE Trans. Energy Convers., vol. 21, no. 1, pp. 130–135, Mar. 2006.
[4] J. Dai, D. Xu, and B. Wu, "A novel control scheme for current–source–converter-based PMSG wind energy conversion systems," IEEE Trans.Power Electron., vol. 24, no. 4, pp. 963–972, Apr. 2009.
[5] J. Birk and B. Andresen, "Parallel-connected converters for optimizingefficiency, reliability and grid harmonics in a wind turbine," in Proc.EPE'07 Conf., Aalborg, Denmark, Sep. 2007, pp. 1–7.
[6] Z. Xu, R. Li, H. Zhu, D. Xu, and C. H. Zhang, "Control of parallel multipleconverters for direct-drive permanent-magnet wind power generationsystems," IEEE Trans. Power Electron., vol. 27, no. 3, pp. 1250–1270,Mar. 2012.
[7] W. Erdman and M. Behnke, "Low wind speed turbine project phase II: Theapplication of medium-voltage electrical apparatus to the class of variablespeed multi-megawatt low wind speed turbines," San Ramon, CA, USA,Natl. Renew. Energy Lab. Rep., NREL/SR-500-38686, Nov. 2005.
[8] H. Abu-Rub, J. Holtz, J. Rodriguez, and G. Baoming, "Medium-voltagemultilevel converters-state of the art, challenges and requirements inindustrial applications," IEEE Trans. Ind. Electron., vol. 57, no. 8,pp. 2581–2596, Aug. 2010.
[9] R. C. Portillo, M. M. Prats, J. I. Leon, J. A. Sanchez, J. M. Carrasco,E. Galvan et al., "Modelling strategy for back-to-back three-level convertersapplied to high-power wind turbines," IEEE Trans. Ind. Electron.,vol. 53, no. 5, pp. 1483–1491, Oct. 2006.
[10] E. J. Bueno, S. Cóbreces, F. J. Rodríguez, A. Hernández, and F. Espinosa,"Design of a back-to-back NPC converter interface for wind turbines withSquirrel-cage induction generator," IEEE Trans. Energy Convers., vol. 23,no. 3, pp. 932–945, Sep. 2008.
[11] A. Faulstich, J. K. Steinke, and F. Wittwer, "Medium voltage converter forpermanent magnet wind power generators up to 7 MW," in Proc. EPEConf., Barcelona, Spain, Sep. 2009, pp. 9–17.
[12] C. L. Xia, X. Gu, and Y. Yan, "Neutral-point potential balancing of threelevelinverters in direct-driven wind energy conversion system," IEEETrans. Energy Convers., vol. 26, no. 1, pp. 18–29, Mar. 2011.
[13] M. Winkelnkemper, F. Wildner, and P. K. Steimer, "6 MVA five-levelhybrid converter for wind power," in Proc. IEEE PESC'08 Conf., Rhodes,Greece, Jun. 2008, pp. 4532–4538.
[14] X. Yuan, J. Chai, and Y. Li, "A transformer-less high-power converter forlarge permanent magnet wind generator systems," IEEE Trans. Sustain.Energy, vol. 3, no. 3, pp. 318–329, Jul. 2012.
[15] C. Xia, Z. Wang, T. Shi, and Z. Song, "A novel cascaded boost chopper forthe wind energy conversion system based on the permanent magnetsynchronous generator," IEEE Trans. Energy Convers., vol. 28, no. 3,pp. 512–522, Sep. 2013.
[16] C.H. Ng,M. A. Parker, R. Li, P. J. Tavner, J. R. Bumby, and E. Spooner, "Amultilevelmodular converter for a large lightweightwind turbine generator,"IEEE Trans. Power Electron., vol. 23, no. 3, pp. 1062–1074, May 2008.
[17] M. A. Parker, C. H. Ng, and L. Ran, "Fault-tolerant control for a modulargenerator converter scheme for direct drive wind turbines," IEEE Trans.Ind.Electron., vol. 58, no. 1, pp. 305–315, Jan. 2011.
[18] J. Kang, N. Takada, E. Yamamoto, and E. Watanabe, "High power matrixconverter for wind power generation applications," in Proc. ICPE ECCEAsia Conf., Jeju, Korea, Jun. 2011, pp. 1331–1336.
[19] M. A. Perez, J. R. Espinoza, J. R. Rodriguez, and P. Lezana, "Regenerativemedium voltage AC drive based on a multi-cell arrangement with reducedenergy storage requirements," IEEE Trans. Ind. Electron., vol. 52, no. 1,pp. 171–180, Feb. 2005.
[20] S. Inoue and H. Akagi, "A bi-directional isolated dc–dc converter as a corecircuit of the next-generation medium-voltage power conversion system,"IEEE Trans. Power Electron., vol. 22, no. 2, pp. 535–542, Mar. 2007.
[21] F. Iov, F. Blaabjerg, J. Clare, O. Wheeler, A. Rufer, and A. Hyde,"UNIFLEX-PM-A key-enabling technology for future European electricitynetworks," EPE J., vol. 19, no. 4, pp. 6–16, 2009.
[22] J. Rodriguez, S. Bernet, B. Wu, J. O. Pontt, and S. Kouro, "Multilevelvoltage source converter topologies for industrial medium-voltage drives,"IEEE Trans. Ind. Electron., vol. 54, no. 6, pp. 2930–2945, Dec. 2007.
[23] H. D. Bang, R. P. Roojj, A. S. McDonald, and M. A. Mueller, "10MWwindturbine direct drive generator design with pitch or active speed stall control,"in Proc. IEEE IEMDC Conf., Antalya, Turkey, vol. 2, May 2007,pp. 1390–1395.
[24] X. Yuan, F. Wang, D. Boroyevich, Y. Li, and R. Burgos, "Dc-link voltagecontrol of a full power converter for wind generator operating in weak-gridsystems," IEEE Trans. Power Electron., vol. 24, no. 9, pp. 2178–2192,Sep. 2009.
[25] R. Cardenas and R. Pena, "Sensor less vector control of induction machinesfor variable-speed wind energy applications," IEEE Trans. Energy Convers.,vol. 19, no. 1, pp. 196–205, Mar. 2004.
[26] P. J. Tavner, G. J. W. Bussel, and F. Spinato, "Machine and converterreliabilities in wind turbines," in Proc. IET PEMD'06 Conf., Dublin,Ireland, Mar. 2006, pp. 127–130.

[27] R. Teodorescu, F. Blaabjerg, M. Liserre, and P. C. Loh, "Proportionalresonantcontrollers and filters for grid-connected voltage–sourceconverters," IEE Proc. Elect. Power Appl., vol. 153, no. 5, pp. 750–762,Sep. 2006.
[28] R. Teodorescu,M. Liserre, and P. Rodriguez, Grid Converters for Photovoltaicand Wind Power Systems, Chap. 4. Hoboken, NJ, USA: Wiley, 2011.
[29] IGBT module datasheet [Online]. Available: http://www.infineon.comdgdl/
[30] S. Dieckerhoff, S. Bernet, and D. KrugPower, "Loss-oriented evaluation ofhigh voltage IGBTs and multilevel converters in transformerless tractionapplications," IEEE Trans. Power Electron., vol. 20, no. 6, pp. 1328–1336,
Nov. 2005.